Blind Reconstruction and Automatic Modulation Classifier for Non-Uniform Sampling Based Wideband Communication Receivers

Student Name: Himani Joshi

IIIT-D-MTech-ECE
July 14, 2016

Indraprastha Institute of Information Technology
New Delhi

Thesis Committee

Dr. Sumit Jagdish Darak (Advisor)
Dr. Anand Srivastava (Internal Reviewer)
Dr. Swades De (External Reviewer, IIT-Delhi)

Submitted in partial fulfillment of the requirements
for the Degree of M.Tech. in Electronics & Communication

Keywords: Automatic Modulation Classifier, Blind Reconstruction, Non-Uniform Sampling, Orthogonal Matching Pursuit.

Certificate

This is to certify that the thesis titled "**Blind Reconstruction and Automatic Modulation Classifier for Non-Uniform Sampling Based Wideband Communication Receivers**" submitted by **Himani Joshi** for the partial fulfillment of the requirements for the degree of *Master of Technology in Electronics and Communication Engineering* is a record of the bonafide work carried out by her under my guidance and supervision at Indraprastha Institute of Information Technology, Delhi. This work has not been submitted anywhere else for the reward of any other degree.

July, 2016

Dr. Sumit J Darak
Assistant Professor
Department of Electronics and Communication
Indraprastha Institute of Information Technology Delhi
New Delhi, 110020

Abstract

Electromagnetic spectrum is a limited natural resource and needs to be used efficiently. However, various measurements conducted worldwide have observed poor spectrum utilization. Software defined radios (SDRs) and cognitive radios (CRs) technologies allow efficient utilization of spectrum by empowering mobile devices to change their transmission parameters like frequency band, sampling rate, modulation scheme, etc. to meet the desired quality of service for different channel conditions. These mobile devices require smart receiver to detect transmission parameters of received signal. Such smart receivers, also known as multi-standard wireless communication receivers (MWCRs), must be capable of digitizing wideband signal ranging from 400 MHz to few GHz to support wide variety of data intensive services. Limited reconfigurability of analog front-end and unavailability of high rate analog to digital converters (ADCs) have generated significant interest in non-uniform (sub-Nyquist) sampling (NUS) and digital reconstruction based MWCRs. Existing reconstruction approaches require prior knowledge of sparsity which may not be available in dynamic spectrum environment. To alleviate this problem, a blind adaptive orthogonal matching pursuit (AOMP) reconstruction approach has been proposed and is the first contribution of this thesis. Novelty of AOMP is the use of online learning algorithm to find spectrum occupancy (i.e. sparsity). Simulation results show that the average reconstruction error of AOMP is 29.7% lower than other approaches.

To validate the usefulness of proposed approach in real life applications, performance of cumulant and machine learning based automatic modulation classifier (AMC) is analyzed for the wideband signal digitized using the proposed approach. The simulation results are further verified on the proposed USRP testbed in real radio environment. Simulation and experimental results show that the accuracy of NUS based AMC approaches the accuracy of uniform sampling based AMC for higher values of SNR and proposed AOMP is superior to others. Also, the performance of AMC does not degrade significantly with NUS given that wideband signal is sparse in frequency.

Acknowledgments

It gives me immense pleasure to express my heartily gratitude to everyone who supported and guided me in the completion of my thesis.

Foremost, I would like to express my sincere gratitude to my advisor Dr. Sumit J Darak. Without his excellent guidance, encouragement and support, I would never be able to finish my thesis work. He has been a great source of inspiration and I feel extremely fortunate to work with him.

I would like to thank Shanon lab technical staff, Mr. Khagendra Joshi and Mr. Rahul Gupta for providing me quick access to all instruments whenever I needed them.

I would like to acknowledge my parents and friends for encouraging and supporting me. They have been a source of moral support to me and have extended their helping hands without fail.

Contents

List of Figures

List of Tables

List of abbrevation

ADC	Analog to Digital Converter
AFE	Analog Front End
AMC	Automatic Modulation Classifier
AOMP	Adaptive Orthogonal Matching Pursuit
BPSK	Binary Phase Shift Keying
CRs	Cognitive Radios
DFE	Digital Front End
DFT	Discrete Fourier Transform
EOMP	Extended Orthogonal Matching Pursuit
IDFT	Inverse Discrete Fourier Transform
IF	Intermediate Frequency
GPABP	Greedy Pursuit Assisted Basis Pursuit
KNN	K-Nearest Neighbor
MCS	Multi-Coset Sampling
MMV	Multiple-Mearsurement Vector
MOMP	Multi-variate Orthogonal Matching Pursuit
MUSIC	Multiple Signal Classification
MWC	Modulated Wideband Converter
MWCRs	Multi-Standard Wireless Communication Receivers
NMSE	Normalized Mean Square Error
NUS	Non-Uniform Sampling
QAM	Quadrature Amplitude Modulation
OMP	Orthogonal Matching Pursuit
QPSK	Quadrature Phase Shift Keying
RF	Radio Frequency
SC-NUS	Single Channel Non-Uniform Sampling
SDR	Software Defined Radio
SFS	Sequential Forward Selection
SNR	Signal to Noise Ratio
SVM	Support Vector Machine
USRP	Universal Software Radio Peripheral

Chapter 1

Introduction

1.1 Motivation

Software defined radios (SDRs) and cognitive radios (CRs) build an intelligent wireless communication system. Evolution of SDRs and CRs allow mobile devices to reconfigure their transmission parameters such as frequency band, modulation type, symbol rate etc. to meet the desired quality of service for any given transmission requirements and channel conditions [1, 2]. Hence, mobile devices need multi-standard wireless communication receivers (MWCRs) to receive signals of different communication standards and estimate their transmission parameters.

A feasible architecture of MWCR, shown in Fig. 1.1, consists of three blocks: 1) analog front-end (AFE), 2) analog-to-digital converter (ADC), and 3) digital front-end (DFE). AFE performs impedance matching, anti-aliasing filtering and applies radio frequency (RF) to intermediate frequency (IF) conversion on a wideband RF signal received by an antenna. This IF signal is then digitized by an ADC and then passed to the DFE. DFE performs two tasks: 1) Digital filtering and 2) Digital Signal processing. Digital filtering shifts the desired frequency band to baseband to perform appropriate sample rate conversion and reconstruction. Digital signal processing involves various signal processing operations such as modulation classification, frequency band detection etc. on the received baseband signal. For SDRs and CRs, MWCR needs to work for all

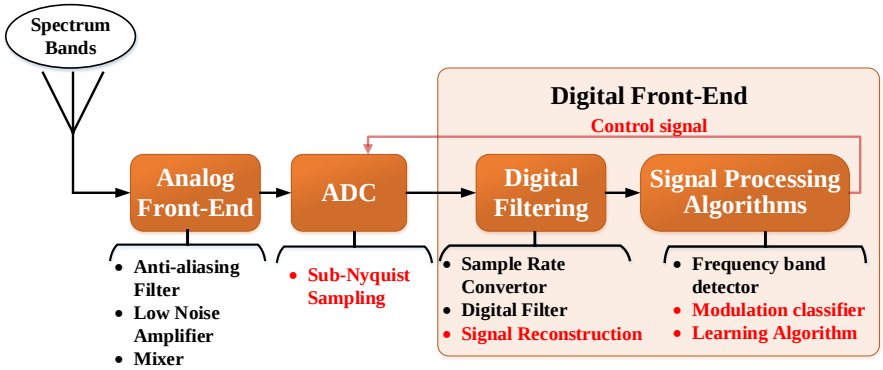

Figure 1.1: Block diagram of multi-standard wireless communication receiver

present and future generation mobile communication standards. But limited reconfigurability of AFE restricts the working of MWCR, hence, ADC should be moved as close to antenna as possible. Without AFE, ADC needs to directly sense the wideband RF spectrum ranging from 400 MHz to few GHz. This is not feasible with existing ADCs due to their huge area, high cost, limited speed and dynamic range requirements. To overcome this problem, various non-uniform (or sub-Nyquist) sampling (NUS) techniques [4–7] have been proposed. Next task after NUS is to develop a reconstruction approach that can accurately reconstruct the signal. Many reconstruction approaches [8–17] developed so far require the prior knowledge of spectrum either in the form of spectrum occupancy (i.e. sparsity) or number of active frequency bands (i.e. active users) in the spectrum. So, there is a need of reconstruction approach which does not require any spectrum knowledge for the reconstruction. The design and implementation of such blind reconstruction approach is the focus of the work presented in this thesis.

1.2 Objectives and Contributions

The objectives of the work presented in thesis are :

1. To develop a low complexity blind reconstruction approach which does not require any prior knowledge of spectrum and performs reconstruction with minimum reconstruction error.

2. To develop automatic modulation classifier (AMC) for non-uniformly sampled and subsequently reconstructed wideband received signal.

3. To develop USRP testbed for performance evaluation of AMC using real radio signals.

Contributions of this thesis, which are under review and submission are described below:

1. H. Joshi, S. J. Darak and Y. Louët, "Blind and Adaptive Reconstruction Approach for Non-Uniformly Sampled Wideband Signal," 5^{th} *International Conference on Advances in Computing, Communications and Informatics (ICACCI)*, Jaipur, India, Sept. 2016.

   In this paper, an adaptive blind reconstruction approach for non-uniformly sampled sparse wideband signal has been proposed. Blind and adaptive nature of proposed approach is implemented by an online learning algorithm. Furthermore, performance comparison of various reconstruction approaches is also made for AMC application.

2. H. Joshi, S. J. Darak and Y. Louët, "Testbed and Experimental Analysis of Automatic Modulation Classifier for Non-uniformly Sampled Signal," submitted in *10th IEEE International Conference on Advanced Networks and Telecommunications Systems (ANTS)*, Bangalore, India, Nov. 2016.

   In this paper, an USRP testbed has been developed to analyze the performance of cumulant based AMC in real radio environment. In the proposed testbed, modulation classification is

performed on either uniformly sampled signal or non-uniformly sampled and subsequently reconstructed signal. For NUS, MCS and OMP based approach is realized.

3. Journal paper, "Blind Reconstruction and Automatic Modulation Classifier for Non-Uniform Sampling Based Wideband Communication Receivers," is under submission.

   In this paper, the detailed description of proposed adaptive blind reconstruction approach for non-uniform sampling is presented. Performance comparison of proposed reconstruction approach is made with other reconstruction approaches for wide range of SNRs and various levels of sparsity. For real life application, cumulant and machine learning classifier based AMC has been developed. This AMC can classify BPSK, QPSK, 16-QAM and 64-QAM modulation schemes from a signal reconstructed by non-uniform samples. Furthermore, to validate the performance of AMC on real radio signal, an USRP testbed of AMC is also developed to classify modulation schemes by both uniform and non-uniform sampling.

1.3 Organization

The thesis is organized as follows. Chapter 2 presents the detailed literature review of various NUS techniques and reconstruction approaches. In Chapter 3, a new adaptive blind reconstruction approach for non-uniformly sampled sparse wideband signal is presented. Later, complexity comparisons of proposed reconstruction approach with other reconstruction approaches are presented. Chapter 4 presents an AMC for non-uniformly sampled and subsequently reconstructed wideband signal. Performance comparison is made between proposed and other reconstruction approaches for wide range of SNRs, different classifiers and various levels of sparsity. In Chapter 5, proposed USRP testbed is discussed. Finally, Chapter 6 concludes the work done in this thesis and briefly discusses the possible future works.

Chapter 2

Literature Review: Non-Uniform Sampling and Reconstruction

Multi-standard wireless communication receivers (MWCRs) described in Chapter 1 require non-uniform sampler and accurate reconstruction technique for wideband signal processing. Detailed review of existing non-uniform sampling (NUS) and reconstruction techniques is done in this chapter.

2.1 Non-Uniform Sampling

Digitization of a wideband RF signal requires ADC of few GHz Nyquist rate and existing ADCs can not meet such a high rate requirement. NUS allows digitization of a wideband RF signal with moderate rate ADCs. If NUS technique selects M samples from N Nyquist rate samples having Nyquist rate of f_{nyq} then, average sampling rate is defined as

$$f_{avg} = \frac{M}{N} \times f_{nyq} \tag{2.1}$$

Next, various NUS techniques are discussed in detail.

2.1.1 Single-Channel Non-Uniform Sampling (SC-NUS)

SC-NUS technique, as shown in Fig. 2.1, randomly selects M samples from N Nyquist rate samples [6]. As the wideband signal, $x(t)$ is sparse in frequency domain, DFT of Nyquist rate samples is recovered via

$$\mathbf{y} = \mathbf{Ax} = \mathbf{D}.\mathbf{F}_N.\mathbf{x} \tag{2.2}$$

where $\mathbf{y} \in \mathbf{R}^{M\times 1}$ is a vector of non-uniform samples, $\mathbf{D} \in \mathbf{Z}^{M\times N}$ is a decimation matrix that selects M samples according to random sample pattern, $\mathbf{F}_N \in \mathbf{C}^{N\times N}$is the IDFT matrix and $\mathbf{x} \in \mathbf{C}^{N\times 1}$ is the DFT of unknown Nyquist rate samples.

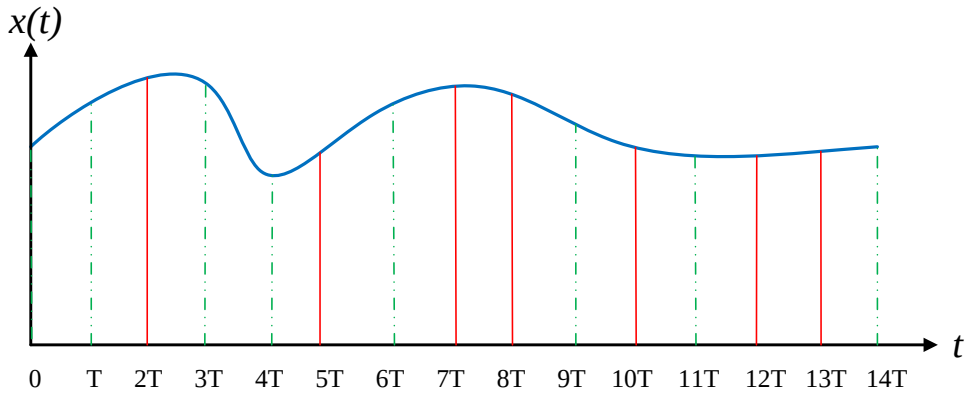

Figure 2.1: Random sample pattern {2,5,7,8,10,12,13} in SC-NUS

2.1.2 Multi-Coset Sampling (MCS)

MCS [4] is a periodic NUS technique. In MCS, an analog wideband signal having Nyquist interval of T, is uniformly sampled by p parallel ADCs. The sampling rate of each ADC is L times lower than the Nyquist rate and each ADC has distinct time offset w.r.t. initial sample which is denoted by sampling pattern, $c_i \in \{1, 2, ..L\}$. Then, the signal at the output of i^{th} ADC is given by [4]

$$x_i(n) = x(nT) \sum_{m \in Z} \delta(n - (mL + c_i)) \qquad 0 \leq i < p \tag{2.3}$$

where L is the sampling period of MCS. Discrete time Fourier transform of each active coset, $x_i(n)$, shown in Fig. 2.2 is a continuous function of frequency.

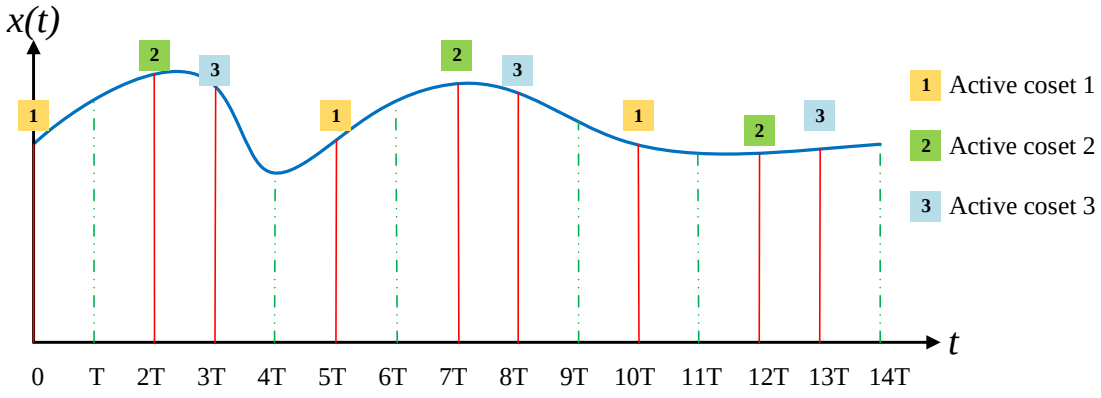

Figure 2.2: MCS for sampling pattern, $c_i = \{0, 2, 3\}$ and $(L,p) = \{5,3\}$

$$\begin{aligned} X_i(e^{j2\pi fT}) &= \sum_{n=-\infty}^{+\infty} x_i(n) \exp(-j2\pi nfT), \\ &= \frac{1}{LT} \sum_{l=0}^{L-1} X\left(f + \frac{l}{LT}\right) \exp\left(\frac{j2\pi c_i l}{L}\right) \end{aligned} \tag{2.4}$$

Hence, input and output can be represented as linear system

$$\mathbf{y}(f) = \mathbf{A}\mathbf{x}(f) \qquad \forall f \in \left[0, \frac{1}{LT}\right) \tag{2.5}$$

where $\mathbf{y}(f)$ is a vector of length p with i-th entry $X_i(e^{j2\pi fT})$, $\mathbf{A}$ is $p \times L$ matrix with $\frac{1}{LT}\exp\left(\frac{j2\pi c_i l}{L}\right)$ as its (i,l)-th entry and $\mathbf{x}(f)$ is a vector of length L with $X\left(f + \frac{l}{LT}\right)$ as its l-th entry. In the above problem $\mathbf{y}(f)$ is a continuous function of frequency hence, finding $\mathbf{x}(f)$ is an infinite dimensional problem. Discrete MCS has been formulated in [6] which finds unknown DFT by finite dimensional multiple measurement vector(MMV) as

$$\mathbf{Y} = \mathbf{A}\mathbf{X} \tag{2.6}$$

where

$$\begin{aligned}
\mathbf{Y} &= \begin{pmatrix} \mathbf{Y}_1 \\ . \\ . \\ . \\ \mathbf{Y}_p \end{pmatrix} \circ \begin{pmatrix} \alpha_{1,1} & . & . & . & \alpha_{1,W} \\ . & . & . & . & . \\ . & . & . & . & . \\ . & . & . & . & . \\ \alpha_{p,1} & . & . & . & \alpha_{p,W} \end{pmatrix} \\
\alpha_{p,w} &= \exp\left[\frac{-2\Pi j.c_i.(w-1)}{N}\right], m \in \{1, ..., W\} \\
\mathbf{X} &= \begin{pmatrix} X(1) & . & . & . & X(W) \\ . & . & . & . & . \\ . & . & . & . & . \\ . & . & . & . & . \\ X((L-1).W+1) & . & . & . & X(L.W) \end{pmatrix}
\end{aligned} \tag{2.7}$$

$\mathbf{Y}_p$ is DFT of p-th active coset and $\circ$ denotes the Hadamard product.

As MCS uses only $M = p.W$ samples out of $N = L.W$ Nyquist rate samples, therefore, average sampling rate is reduced to

$$f_{avg} = \frac{p}{L} \times f_{nyq} \tag{2.8}$$

2.1.3 Modulated Wideband Converter (MWC)

MWC [7] is another NUS technique where the received analog signal, $x(t)$, is multiplied with each of m parallel mixing functions, $p_i(t), 1 \leq i \leq m$, in analog front-end. The $p_i(t)$ is a piecewise continuous function with magnitude of either +1 or -1 and it is periodic with period, $T_p = \frac{1}{f_p}$. Since, $p_i(t)$ is a periodic function, its Fourier series expansion

$$p_i(t) = \sum_{l=-\infty}^{+\infty} c_{il} e^{j\frac{2\pi}{T_p}lt} \tag{2.9}$$

where c_{il} is the Fourier series coefficient.

Thus, as shown in Fig. 2.3, the Fourier transform of the output of i-th channel multiplier can be represented as linear combination of signal spectrum which is shifted by lf_p. This stage is called mixing stage. Mathematically, Fourier transform of the output of mixing stage will be

$$\begin{aligned}\tilde{X}_i(f) &= \int_{-\infty}^{+\infty} x(t) \left(\sum_{l=-\infty}^{+\infty} c_{il} e^{j\frac{2\pi}{T_p}lt} \right) e^{-j2\pi ft} dt \\ &= \sum_{l=-\infty}^{+\infty} c_{il} X(f - lf_p)\end{aligned} \tag{2.10}$$

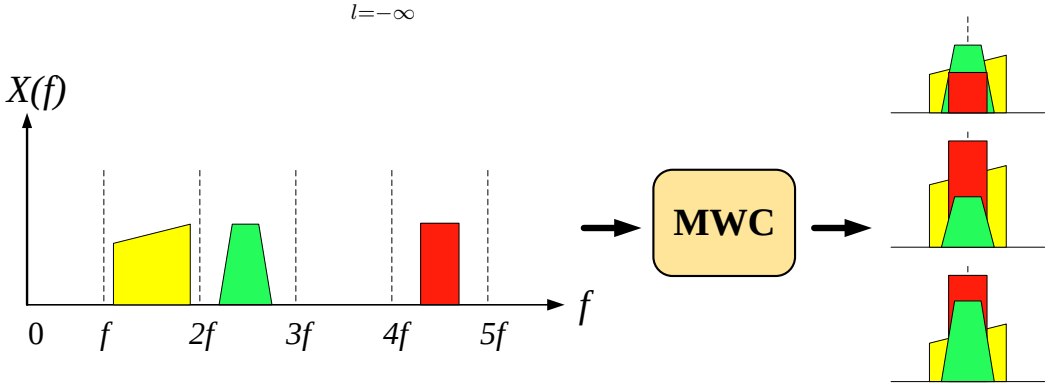

Figure 2.3: Input and output spectrum of three channel MWC

After this, MWC has filtering stage which performs low pass filtering to bandlimit the aliased signal to $[-f_s/2, f_s/2]$. ADC of each branch then performs uniform sampling at rate of $f_s = \gamma f_p$ where $\gamma \in \mathbb{Z}$ is known as collapsing factor. Therefore, the relation between discrete time Fourier transform of these known samples and $X(f)$ is

$$\mathbf{Y}_i(e^{j2\pi fT_s}) = \sum_{l=-L_o}^{+L_o} c_{il} \mathbf{X}(f - lf_p), \quad f \in [-f_s/2, +f_s/2] \tag{2.11}$$

where L_o is the smallest integer that takes the contribution of all non-zero frequency sub-bands and hence total number of frequency sub-bands, $L = 2L_o + 1$.

In matrix form, equation 2.11 can be represented as a linear system of m equations

$$\mathbf{y}(f) = \mathbf{A}\mathbf{z}(f) \tag{2.12}$$

where $\mathbf{A}$ is $m \times L$ matrix with $\mathbf{A}_{il} = c_{il}*$, $\mathbf{y}$(f) is a vector of m elements with $\mathbf{Y}_i(e^{j2\pi fT_s})$ as its i-th element and $\mathbf{z}$(f) is a vector of L elements with $\mathbf{X}(f - lf_p)$ as its l-th element. Above equation is a continuous function of frequency, so, it becomes an infinite measurement vector problem. It can be converted into MMV problem by using continuous to finite (CTF) process [7].

In the rest of thesis, each row of $x(f)$ and $z(f)$ of Eq.2.5 and 2.12, respectively, is referred as sub-band. Furthermore, occupied and vacant sub-bands are referred as active and vacant

sub-bands, respectively.

Each NUS technique has its own advantages and disadvantages. SC-NUS is the simplest but random selection of sample pattern leads to the requirement of high Nyquist rate ADC. MCS uses multiple moderate rate ADCs in parallel but requires accurate time shift of the order of T. Such time shifts are difficult to achieve in hardware and hence, may lead to significant reconstruction error. MWC does not require such a small time shift and it has been implemented on hardware in [7]. However, it uses analog front end for NUS.

2.2 Reconstruction Approaches

Next step after NUS is to accurately reconstruct the original signal from non-uniform samples. In [9], error bounds on the peak value and energy of aliasing errors are calculated and further, conditions for perfect reconstruction are derived. However, this method requires the information of spectral support of multiband signal which can not be available in practice.

Spectrum blind reconstruction (SBR) approach [10] performs reconstruction in two stages. Initially, it transforms the continuous system given in Eq 2.12 into a finite dimensional problem without performing discretization and then applies multiple-mearsurement vector (MMV) solver. In [11, 12], authors used blind sequential forward selection (SFS) algorithm to find sampling pattern for MCS. For reconstruction, information theoretic criteria along with multiple signal classification (MUSIC) algorithm (explained later) is used in [11] whereas non-linear least square estimator is used in [12]. Reconstruction approaches proposed in [10–12] require the knowledge of spectrum occupancy (i.e. sparsity) which is not readily available.

In [8], K sets of sampling pattern are randomly selected and then worst case condition number is calculated for each set using SFS algorithm. Finally, the set with minimum worst case condition number is selected. For reconstruction, MUSIC algorithm is applied on the correlation matrix of DFT of multi-coset samples.

MUSIC algorithm [13] uses Eigen space approach to reconstruct unknown m-sparse signal i.e. the signal which contains maximum m non zero elements. From the Eigen value decomposition of $\mathbf{Y}$ of Eq. 2.6, m Eigen vectors corresponding to m largest Eigen values span signal subspace. Remaining Eigen vectors span the orthogonal subspace and correspond to noise. Then location of active sub-bands is calculated as

$$P_{MU}(k) = \frac{1}{\|\mathbf{a}_k \hat{\mathbf{E}}_n\|^2}, \quad 0 \leq k \leq (L-1) \tag{2.13}$$

where $\mathbf{a}_k$ is the k^{th}column of $\mathbf{A}$ and $\hat{\mathbf{E}}_n$ is a matrix containing noise Eigen vectors. MUSIC is non-iterative approach and hence less complex.

Multi-variate orthogonal matching pursuit (MOMP) [14, 15] is an iterative algorithm and at each iteration it finds one non-zero entry of m-sparse signal. Thus, for finding the approximate

solution, MOMP requires m iterations. Greedy pursuits assisted basis pursuits (GPABP) [16] finds the support vector in two steps. First, it finds the common support from any two greedy algorithms and then applies modified basis pursuit (Mod-BP) [18]. Due to the use of multiple algorithms, computation complexity of GPABP is very high. Recently, extended OMP (EOMP) has been proposed in [17]. It uses more than m-iterations for finding correct active sub-bands and hence, it is more robust than OMP. Reconstruction approaches discussed in [8, 13–17] use the information of number of active sub-bands for the reconstruction. Thus, all reconstruction approaches [8–17] used for the reconstruction of sparse wideband signal either require the knowledge of sparsity or number of active sub-bands.

2.3 Summary

In this chapter, various NUS and reconstruction approaches proposed in literature are discussed. Due to the use of moderate rate ADCs, MCS and MWC are widely studied NUS techniques. Reconstruction approaches studied in literature require the knowledge of spectrum either in terms of spectrum occupancy or number of active sub-bands and their location. Hence, these reconstruction approaches are not completely blind. Design of low complexity blind reconstruction approach for MWCRs is the focus of work presented in this thesis.

Chapter 3

Blind and Adaptive Reconstruction Approach for Non-Uniformly Sampled Wideband Signal

In this chapter, an adaptive blind reconstruction approach for non-uniformly sampled sparse wideband signal has been proposed. The term blind indicates that the proposed approach does not require any prior knowledge of number of active frequency bands (i.e. active users) in the spectrum of received signal. While the term adaptive means that the parameters are dynamically tuned based on spectrum occupancy estimated via online learning algorithm. Since the proposed approach is based on Orthogonal Matching Pursuit (OMP) method, it shall be referred to as Adaptive OMP (AOMP).

3.1 Proposed AOMP Reconstruction Approach

The desired characteristics of reconstruction technique are:

1. It should be blind.
2. Reconstruction error should be as low as possible especially at low SNR.
3. Reconstruction approach should be independent of location of active sub-bands.
4. Computational complexity should be as minimum as possible.

Reconstruction of a sparse wideband spectrum, $\mathbf{X}$ of different NUS techniques discussed in Chapter 2 can be performed by solving following linear system

$$\mathbf{Y} = \Phi.\mathbf{D}.\mathbf{X} \tag{3.1}$$

where $\mathbf{Y} \in \mathbb{C}^{p \times L}$ with $p < L$ is either non-uniform samples or function of non-uniform samples, $\Phi \in \mathbb{R}^{p \times L}$ is a decimation matrix, $\mathbf{D} \in \mathbb{C}^{L \times L}$ is a dictionary matrix and $\mathbf{X} \in \mathbb{C}^{L \times W}$ is sparse spectrum of wideband signal or its function. Eq. 3.1 can be re-written as

$$\mathbf{Y} = \mathbf{A}.\mathbf{X} \tag{3.2}$$

where $A = \Phi.\mathbf{D}$.

For the reconstruction of $m-$sparse $\mathbf{X}$ from $\mathbf{Y}$, matrix $\mathbf{A}$ should satisfy the Restricted Isometry Property (RIP) [19] of order m. A matrix $\mathbf{A}$ satisfies RIP of order m if for an isometry constant, $\delta_m \in (0, 1)$

$$(1 - \delta_m \|\mathbf{X}\|_2^2) \leq \|\mathbf{A}.\mathbf{X}\|_2^2 \leq (1 + \delta_m \|\mathbf{X}\|_2^2) \tag{3.3}$$

Eq. 3.3 implies, the matrix $\mathbf{A}$ approximately preserves the Euclidean length of m-sparse $\mathbf{X}$ which means, all m columns of $\mathbf{A}$ are nearly orthogonal.

In the case of NUS techniques discussed in Chapter 2, matrix $\mathbf{A}$ is a combination of decimation matrix, Φ and partial Fourier matrix, $\mathbf{D}$. It has been shown in [20] that such matrix holds RIP and hence, can reconstructs $\mathbf{X}$ with high probability.

Reconstruction of a sparse wideband spectrum can be performed by two methods: 1) l-1 minimization method, and 2) Iterative method. l-1 minimization method can stably recovers the sparse signal but it has high computational cost and implementation complexity. It is shown in [14] that OMP, which follows iterative method, can recovers m-sparse signal with low computational cost and implementation complexity if number of measurements, p are nearly proportional to m. In this thesis, the proposed reconstruction approach, AOMP, is based on well known OMP approach. OMP approach [14], rather than any reconstruction approach, can stably recovers m-sparse signal if the measurement matrix, $\mathbf{A}$, satisfies RIP of order m. OMP is non-blind iterative algorithm where number of iterations depend on the number of non-zero values of signal. In each iteration, OMP finds a column of measurement matrix, $\mathbf{A}$, which is strongly correlated with the received signal. At the end of m^{th} iteration, m such columns of $\mathbf{A}$ lead to the reconstruction of original signal.

The proposed AOMP approach is shown in Algorithm 1. It finds the solution in k number of iterations where k is defined by learned spectrum occupancy, $\bar{\Omega}$ and normalized SNR, α. Value of $\bar{\Omega}$ is estimated using online learning algorithm while value of α can be easily estimated at receiver by measuring noise in any vacant frequency sub-band.

First step in AOMP approach is to find number of active sub-bands in the received wideband spectrum. To do this, AOMP estimates the spectrum occupancy, $\bar{\Omega}$ using online learning algorithm, named Upper Confidence Bound (UCB) algorithm [21, 22]. The UCB is a sequential algorithm which selects subset of frequency sub-bands depending on their quality index in each iteration. The quality index is given by [21],

$$G_u(v, l_u) = \frac{D_u(v, l_u)}{T_u(v, l_u)} + \sqrt{\frac{\mu \cdot \ln(v)}{T_u(v, l_u)}} \tag{3.4}$$

where v is iteration number, l_u is the sub-band index, $G_u(v, l_u)$ is quality index of sub-band l_u at iteration v, $T_u(v, l_u)$ is the number of times the sub-band l_u is chosen up to iteration v, $D_u(v, l_u)$ is the number of times sub-band l_u is observed as active up to iteration v and μ is exploration constant. In order to accurately and quickly estimate $\bar{\Omega}$, μ should be chosen sufficiently large [21]. Then, $\bar{\Omega}$ is given as

$$\bar{\Omega}(v) = \prod_{l_u=1}^{L_u} \frac{D_u(v, l_u)}{T_u(v, l_u)} \tag{3.5}$$

where L_u is the number of frequency sub-bands. UCB algorithm has been mathematically proved to be optimal with logarithmic regret which means that $\bar{\Omega}$ from UCB is very close to actual Ω [21, 22]. Similar behavior has been validated in Fig. 3.1 especially when signal is sparse. Fig. 3.1 shows that for higher spectrum occupancy of 0.4, learned spectrum occupancy becomes almost same as actual spectrum occupancy in less than 15 iterations.

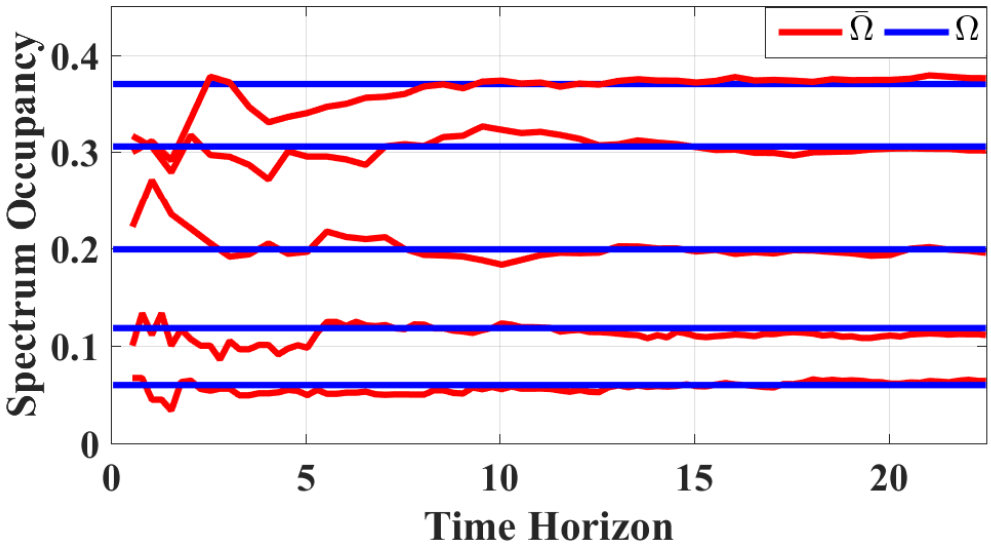

Figure 3.1: Learned and actual value of spectrum occupancy for L_u=20 and μ=10.

For f_{nyq}, Nyquist rate and B_{max}, maximum possible occupied bandwidth of an active frequency band, the number of active sub-bands, m can be calculated as

$$m = \left\lceil \frac{\bar{\Omega}.f_{nyq}}{B_{max}} \right\rceil \tag{3.6}$$

Thus, by finding the number of active sub-bands from spectrum occupancy, AOMP does not require prior knowledge of number of active frequency bands (i.e. active users) in the spectrum and hence, AOMP reconstruction approach is blind in nature.

In AOMP, the number of iterations are not fixed and depend on the values of m and α. This is

because, empirical observations indicate that OMP can not guarantee successful identification of all m active sub-bands in m iterations. Thus, for reducing the reconstruction error at high SNR i.e. for SNR > 0, $\lfloor \alpha m \rfloor$ more supports are generated which increase the accuracy of selecting correct active sub-bands and hence, reduce the reconstruction error. But at low SNR i.e. SNR ≤ 0, selection of vacant sub-bands leads to high reconstruction error. Therefore, for minimizing the reconstruction error at low SNR, AOMP restricts the length of support to m. So, in AOMP, the number of iterations, k, depend on α and m and can be written as

$$k = \begin{cases} m + \lfloor \alpha * m \rfloor & \text{if } \alpha > 0, \\ m & \text{if } \alpha \leq 0. \end{cases} \tag{3.7}$$

Please refer to Preposition 1 which shows that the AOMP selects all m supports in $m + \lfloor \alpha * m \rfloor$ iterations and with 0 residual if measurement matrix $\mathbf{A}$ satisfies RIP of order $m + \lfloor \alpha * m \rfloor$. Furthermore, Preposition 2 supports Preposition 1 by showing that AOMP leads to lower normalized mean square error (NMSE) than MOMP even when the received signal is not fully sparse due to the presence of noise in the vacant sub-bands.

In the following preposition, it is proved that the AOMP can successfully finds any m-sparse signal with zero residual in $m + \lfloor \alpha m \rfloor$ iterations.

Preposition 1. For a linear system $\mathbf{Y} = \mathbf{A}.\mathbf{X}$ where $\mathbf{X} \in \mathbb{C}^{l \times w}$ is a m-sparse signal, $\mathbf{A} \in \mathbb{C}^{p \times l}$ is a measurement matrix which follows RIP of an order $(m + \lfloor \alpha m \rfloor)$ and $\mathbf{Y} \in \mathbb{C}^{p \times w}$ is measurements, AOMP will reconstruct m-sparse signal $\mathbf{X}$ with residual, $\mathbf{R} = 0$ in $(m + \lfloor \alpha m \rfloor)$ iterations iff actual support, $S \subseteq \wedge_{m + \lfloor \alpha m \rfloor}$

Proof : For exact solution, $\mathbf{Y}$ will always span the column space $\mathcal{R}(\mathbf{A}_S)$. As $S \subseteq \wedge_{m+\lfloor \alpha m \rfloor}$, therefore, $\mathbf{Y}$ will also span the column space $\mathcal{R}(\mathbf{A}_{\wedge_{m+\lfloor \alpha m \rfloor}})$. This implies, approximate solution produced at $(m + \lfloor \alpha m \rfloor)^{th}$ iteration will be exact solution. As $\mathbf{A}$ follows RIP of order $m + \lfloor \alpha * m \rfloor$, therefore, $\mathbf{A}(\mathbf{X} - \hat{\mathbf{X}}) = 0$ which means residual at $(m + \lfloor \alpha m \rfloor)^{th}$ iteration will become 0 when $\hat{\mathbf{X}} = \mathbf{X}$.

In Preposition 1, it is assumed that $\mathbf{X}$ is m-sparse which may not always be true especially at low SNR. Preposition 2 shows that the proposed AOMP reconstructs a noisy signal with better NMSE than MOMP for wide range of SNRs.

Preposition 2. For a noisy linear system, $\mathbf{Y} = \mathbf{A}\mathbf{X} + \mathbf{e}$, let $\hat{\mathbf{X}}$ be the reconstructed signal then $\|\mathbf{X} - \hat{\mathbf{X}}\|^2_{2,AOMP} \leq \|\mathbf{X} - \hat{\mathbf{X}}\|^2_{2,MOMP}$ for wide range of SNRs.

Proof: Let S be the original support of the signal. At k^{th} iteration, AOMP selects k^{th} highly correlated column of $\mathbf{A}$. If $k \geq m$, then it implies that AOMP has selected atleast $(k - m)$ additional supports, $\wedge_{k-m} \nsubseteq S$. These additional supports correspond to the vacant sub-bands occupied with noise.Therefore, at low SNR, noise is very high due to which for $k \geq m$ iterations, $\|\mathbf{X} - \hat{\mathbf{X}}\|$ becomes very large. Hence, as shown in Algorithm 1, number of iteration in AOMP approaches m as noise increases. Whereas at high SNR, effect of noise may not be significant and hence, the probability of selecting correct active sub-bands is higher when $k > m$. Hence,

Algorithm 1: AOMP Reconstruction Approach

Input:
- Measurement matrix, $\mathbf{A} \in \mathbb{C}^{P\,X\,L}$
- Preprocessed Measurement, $\mathbf{Y} \in \mathbb{C}^{P\,X\,W}$
- Spectral occupancy, $\overline{\boldsymbol{\Omega}}$
- Normalized SNR, α

Output:
- Estimated signal, $\widehat{\mathbf{X}} \in \mathbb{C}^{L\,X\,W}$
- Support, Λ

Initialize: $\boldsymbol{\Lambda} = \emptyset$, Residual, $\mathbf{R} = \mathbf{Y}$, k = 0,

$$m = \left\lceil \frac{(\overline{\boldsymbol{\Omega}} * f_{nyq})}{B_{max}} \right\rceil$$

$$iter = \begin{cases} m + \lfloor \alpha m \rfloor & if\ \alpha > 0 \\ m & if\ \alpha \leq 0 \end{cases}$$

Procedure:
1. k = k+1
2. $\lambda_k = \arg \max_{j=\{1\ldots.L\}\setminus\Lambda} \left\| \mathbf{A}_j^* \mathbf{R} \right\|_2^2$
3. $\Lambda_k = \Lambda_{k-1} \cup \{\lambda_k\}$
4. $\widehat{\mathbf{X}}_k = \mathbf{A}_{\wedge_k}^{\dagger} \mathbf{R}$
5. $\mathbf{R} = \mathbf{Y} - \mathbf{A}_{\wedge_k} \widehat{\mathbf{X}}_k$
6. Repeat steps 1 to 5 till $k \leq iter$

in the AOMP, we have $\hat{\mathbf{X}}_{\wedge_k} = \mathbf{A}_k^{\dagger}.\mathbf{R_k}$. Furthermore, by increasing the probability of selecting correct active sub-bands, AOMP achieves lower NMSE at high SNR than MOMP.

After obtaining m and k, remaining steps in AOMP are numbered as 1-6 in Algorithm 1. In step 1, AOMP selects the column of $\mathbf{A}$ which is highly correlated to the residual, $\mathbf{R}$. Note that $\mathbf{R}$ is initialized to $\mathbf{Y}$ in the first iteration. In the k^{th} iteration, k^{th} highly correlated column of $\mathbf{A}$ is selected. This index is appended to previously found support, $\wedge_{k-1}$. Then with the help of new support, $\wedge_k$, the approximate solution, $\hat{\mathbf{X}}_k$ is calculated by pseudo-inverse of measurement matrix, $\mathbf{A}_k$ which is having columns corresponding to new support. At the end, residual is updated using approximated solution, $\hat{\mathbf{X}}_k$.

When compared to OMP, AOMP is more complex due to $\lfloor \alpha m \rfloor$ extra iterations and the use of learning algorithm. This is a small penalty paid to make AOMP blind. On the other hand, AOMP requires only $O\left(m \ln \frac{d}{\lfloor \alpha m \rfloor + 1}\right)$ data samples compared to $O(m \ln d)$ samples in case of OMP.

3.2 Simulation Results and Complexity Analysis

In this Section, simulations and complexity results are presented to compare various digital reconstruction approaches for three NUS techniques, namely MCS, MWC and SC-NUS. To

the best of our knowledge, the performance comparison of all NUS techniques with various reconstruction approaches has not been done before in the literature.

3.2.1 Simulation Results

A wideband signal with maximum frequency of 5 GHz is used for simulation. The signal is assumed to be sparse in frequency and consists of N active frequency bands of distinct bandwidth. Note that the bandwidth and location of each active frequency band are chosen randomly. With $L = 19$, $f_p = 50.7$ MHz and $\gamma = 10$, sampling rate of ADCs used in MCS, MWC and SC-NUS is 526 MHz, 507 MHz and 10 GHz, respectively. The exploration coefficient, μ of UCB learning algorithm is fixed to 10 and each numerical result reported hereafter is the average of the values obtained over 100 independent experiments. To validate and compare different reconstruction approaches, NMSE between original signal, $x(t)$ and reconstructed signal $\hat{x}(t)$ is calculated as

$$NMSE = \frac{\|(|x(t)| - |\hat{x}(t)|)\|_2}{\|x(t)\|_2} \tag{3.8}$$

The NMSE of various digital reconstruction approaches is compared for wide range of SNRs and different number of active frequency bands in Fig. 3.2, 3.3 and 3.4 for MWC, MCS and SC-NUS, respectively. From Fig. 3.2, 3.3 and 3.4, it is observed that NMSE decreases with increase in SNR and decrease in the number of active frequency bands. Numerically, AOMP offers an average improvement of 2.12%, 24.09% and 29.70% in NMSE over MOMP, MUSIC and GPABP, respectively. Proposed AOMP performs well for all NUS techniques and produces minimum NMSE for MCS and MWC at low SNR.

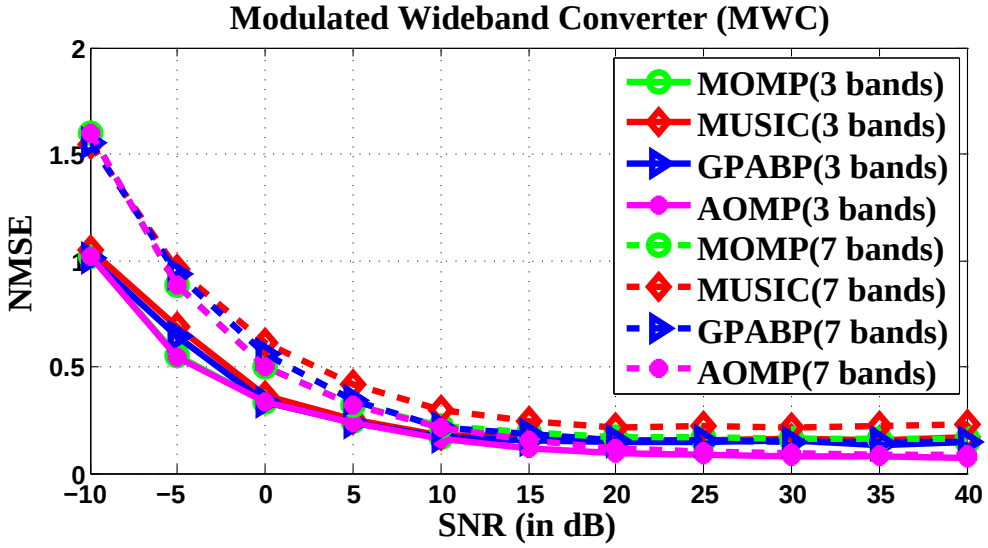

Figure 3.2: NMSE of MWC versus SNR for different number of bands

In Fig. 3.4, MUSIC reconstruction approach has slightly lower NMSE at SNR of -10dB. It happens because MUSIC approach finds frequency samples of active sub-bands with more accuracy than other reconstruction approaches. It is also observed that MUSIC reconstruction approach

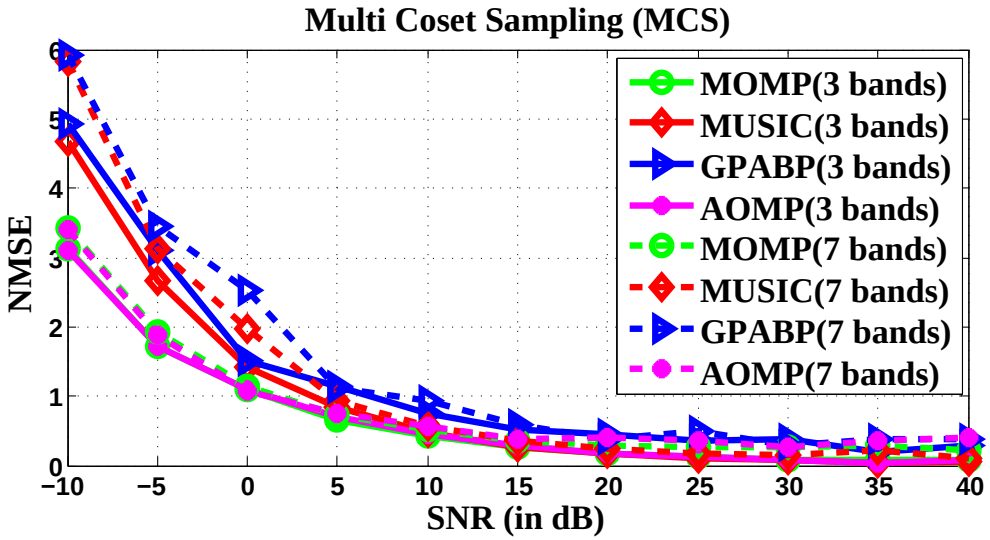

Figure 3.3: NMSE of MCS versus SNR for different number of bands

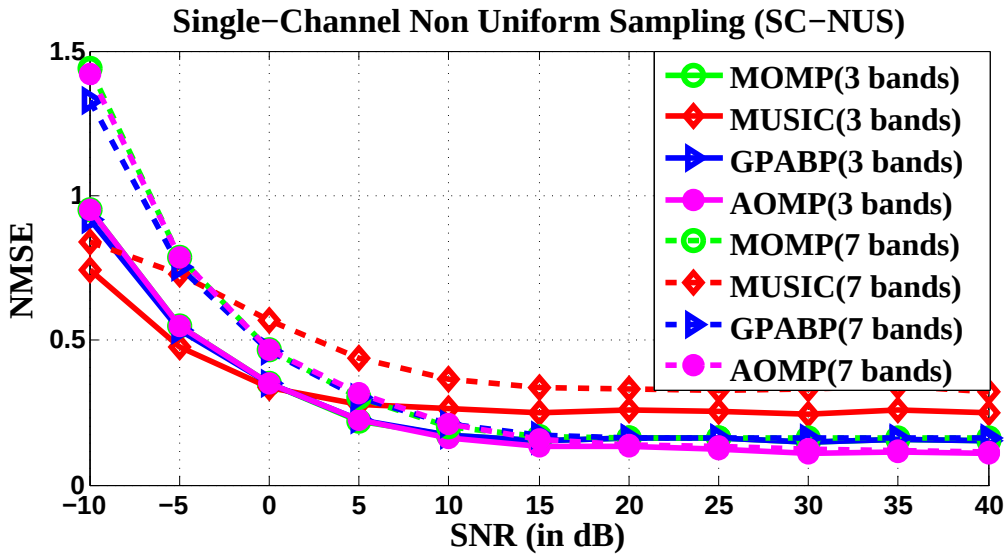

Figure 3.4: NMSE of SC-NUS versus SNR for different number of bands

for SC-NUS has minimum NMSE when compared to other NUS techniques. It happens because in case of MCS and MWC, MUSIC identifies those frequency sub-bands in which active sub-bands are present whereas in SC-NUS, MUSIC identifies frequency samples of active sub-bands. So, if MUSIC detects wrong frequency sub-band in MCS and MWC then entire active sub-band would go undetected and leads to high NMSE whereas in SC-NUS, MUSIC detects some samples of active sub-bands due to which its NMSE is lower than MCS and MWC.

Table 3.1, 3.2 and 3.3 show the NMSE comparison of different reconstruction approaches for MWC, MCS and SC-NUS, respectively. The NMSE comparison is done for various number of active frequency bands over different SNR values. Number of active frequency bands for MWC and SC-NUS is varied from 4 to 20 while the range is 1 to 7 in MCS. The smaller range in MCS is because for $L = 19$, p, which is always greater than $2N$ should be less than L. From Table 3.1,

Table 3.1: NMSE of MWC for different number of bands and SNR

Number of Bands	SNR = -5dB					SNR = 0dB					SNR = 10dB				
	MOMP	MUSIC	EOMP	GPABP	AOMP	MOMP	MUSIC	EOMP	GPABP	AOMP	MOMP	MUSIC	EOMP	GPABP	AOMP
4	0.66	0.77	0.80	0.75	0.66	0.38	0.45	0.45	0.40	0.38	0.20	0.20	0.18	0.19	0.17
6	0.83	0.91	1.00	0.88	0.83	0.45	0.55	0.56	0.50	0.45	0.22	0.23	0.22	0.21	0.19
8	0.95	1.01	1.16	1.00	0.95	0.52	0.67	0.65	0.60	0.52	0.23	0.33	0.24	0.23	0.22
10	1.06	1.12	1.33	1.13	1.05	0.59	0.74	0.74	0.67	0.59	0.25	0.38	0.27	0.25	0.24
12	1.17	1.20	1.48	1.21	1.15	0.68	0.82	0.83	0.76	0.68	0.27	0.45	0.30	0.28	0.27
14	1.28	1.32	1.65	1.32	1.28	0.72	0.88	0.92	0.80	0.72	0.29	0.50	0.33	0.29	0.29
16	1.34	1.43	1.84	1.43	1.39	0.76	0.94	1.01	0.86	0.78	0.35	0.60	0.36	0.35	0.31
18	1.31	1.52	2.02	1.55	1.47	0.80	1.01	1.14	0.93	0.86	0.42	0.63	0.39	0.37	0.34
20	1.36	1.69	2.24	1.67	1.58	0.81	1.09	1.27	1.02	0.92	0.47	0.71	0.43	0.42	0.37

Table 3.2: NMSE of MCS for different number of bands and SNR

Number of Bands	SNR = -5dB					SNR = 0dB					SNR = 10dB				
	MOMP	MUSIC	EOMP	GPABP	AOMP	MOMP	MUSIC	EOMP	GPABP	AOMP	MOMP	MUSIC	EOMP	GPABP	AOMP
1	1.20	1.68	1.53	2.4	1.20	0.73	0.87	0.89	1.38	0.73	0.15	0.15	0.17	0.16	0.16
2	1.60	3.49	1.91	4.75	1.60	0.98	1.56	1.20	2.00	0.98	0.22	0.21	0.25	0.22	0.22
3	1.75	3.08	2.09	3.63	1.74	1.08	1.78	1.27	2.60	1.06	0.28	0.27	0.33	0.33	0.29
4	2.12	2.95	2.28	3.27	2.03	1.29	1.81	1.34	1.99	1.21	0.35	0.33	0.42	0.62	0.36
5	1.99	3.29	2.28	5.03	1.95	1.14	1.61	1.30	1.94	1.11	0.39	0.48	0.43	0.68	0.39
6	1.98	4.41	2.18	2.82	1.95	1.16	2.46	1.23	1.56	1.10	0.64	6.49	0.43	0.97	0.41
7	1.91	2.62	2.20	2.41	1.90	1.10	1.40	1.23	1.65	1.06	0.65	5.8	0.49	0.85	0.49

Table 3.3: NMSE of SC-NUS for different number of bands and SNR

Number of Bands	SNR = -5dB					SNR = 0dB					SNR = 10dB				
	MOMP	MUSIC	EOMP	GPABP	AOMP	MOMP	MUSIC	EOMP	GPABP	AOMP	MOMP	MUSIC	EOMP	GPABP	AOMP
4	0.60	0.58	0.73	0.59	0.60	0.38	0.40	0.45	0.38	0.38	0.17	0.27	0.17	0.17	0.17
6	0.72	0.71	0.86	0.71	0.72	0.44	0.52	0.52	0.43	0.44	0.19	0.31	0.21	0.19	0.20
8	0.82	0.74	1.00	0.79	0.81	0.49	0.62	0.58	0.48	0.48	0.20	0.39	0.23	0.21	0.21
10	0.92	0.76	1.11	0.86	0.92	0.55	0.67	0.65	0.52	0.54	0.23	0.51	0.25	0.23	0.23
12	1.01	0.77	1.21	0.93	0.99	0.59	0.71	0.70	0.57	0.58	0.24	0.58	0.27	0.24	0.25
14	1.08	0.78	1.31	0.98	1.06	0.61	0.73	0.74	0.58	0.61	0.26	0.63	0.29	0.26	0.27
16	1.16	0.79	1.41	1.03	1.15	0.65	0.74	0.78	0.61	0.64	0.27	0.67	0.31	0.27	0.29
18	1.22	0.81	1.47	1.06	1.19	0.70	0.74	0.83	0.64	0.68	0.29	0.69	0.33	0.28	0.30
20	1.30	0.83	1.58	1.12	1.28	0.72	0.75	0.86	0.66	0.70	0.30	0.70	0.33	0.29	0.31

3.2 and 3.3, it can be observed that AOMP offers superior performance over other reconstruction approaches for all three NUS techniques. As discussed in Section 3.1, performance of AOMP remains almost same as that of MOMP when $SNR \leq 0$ and same trait has been seen in Table 3.2 and 3.3. But in Table 3.1, at low SNR of -5dB and 0dB, NMSE of AOMP is slightly higher than MOMP when the number of active frequency bands is more than 14. Degradation in the performance of AOMP occurs because for large number of active frequency bands, the number of predicted active sub-bands from Eq. 3.6 is less than its actual value which is $2N$. On the other hand, in Table 3.3, it can be observed that the performance of AOMP is almost same as that of MOMP even for large number of bands. It happens due to sample based reconstruction nature of SC-NUS which finds samples of active sub-bands. So, from Table3.1,3.2 and 3.3 it can be observed that blind AOMP reconstruction approach performs well for wide range of SNRs and different levels of spectrum occupancy.

3.2.2 Complexity Analysis

Computation complexity of various reconstruction approaches is shown in Table 3.4 and the term NA indicates not applicable. MUSIC algorithm involves norm calculation of multiplication of two vectors for L times, autocorrelation and sorting of a vector for two times, Eigen-value decomposition of $p \times p$ matrix for one time. All these operations are performed once. GPABP algorithm uses the support recovered by MOMP and MUSIC algorithms followed by Mod-BP which uses convex minimization.

Table 3.4: Complexity comparison of reconstruction algorithms

Operations	**Complexity of Operations**	**MOMP [14]**	**EOMP [13]**	**AOMP**	**MUSIC [17]**	**GPABP [16]**
Sorting	$O(n^2)$	–	–	–	2	2
Addition/Subtraction	$O(n)$	$m*(p^2)$	$(m+\lfloor 0.5m \rfloor)*(p^2)$	$(m+\lfloor \alpha m \rfloor)*(p^2)$	–	$m*(p^2)$
Matrix Multiplication	$O(n^3)$	$3m$	$3(m+\lfloor 0.5m \rfloor)$	$3(m+\lfloor \alpha m \rfloor)$	3	$3m+3$
Norm Calculation	$O(3n)$	L	L	L	L	$2L$
Eigen-Value Decomposition	$O(n^3)$	–	–	–	1	1
Least Square Solution	$O(n^2q)$	m	$m+\lfloor 0.5m \rfloor$	$m+\lfloor \alpha m \rfloor$	–	m
Finding Maximum Value	$O(n)$	m	$m+\lfloor 0.5m \rfloor$	$m+\lfloor \alpha m \rfloor$	–	m
Convex Minimization	$O(n^2q^{1.5})$	–	–	–	–	1

As MOMP, EOMP and AOMP are variants of OMP, therefore, their complexity is almost same. All three approaches involve norm calculation of multiplication of two vectors for L times, maximum element detection among a vector, multiplication of two matrices of size $p \times L$ and $L \times W$ and subtraction of $p \times W$ matrix. But they perform these operation for different number of iterations. MOMP needs m number of iterations where m is the number of active sub-bands. EOMP needs $(m + \lfloor \alpha m \rfloor)$ iterations and here we assume that $\alpha = 0.5$. For AOMP, the number of iterations depends on spectrum occupancy and SNR and it is observed that AOMP takes same number of iteration as MOMP for low SNR whereas it is same as EOMP for high SNR. Since, AOMP uses UCB algorithm to estimate the sparsity, the complexity of AOMP is slightly

higher than MOMP and EOMP but significantly lower than GPABP.

3.3 Summary

In this chapter, a low complexity adaptive orthogonal matching pursuit (AOMP) approach has been proposed to blindly reconstruct a sparse wideband signal received at multi-standard wireless communication receivers (MWCRs). The proposed AOMP does not need any knowledge of spectrum and channel quality. Simulation and complexity results verify superiority of the proposed AOMP over existing approaches for three NUS techniques namely multi coset sampling (MCS), modulated wideband converter (MWC) and single channel non-uniform sampling (SC-NUS). Proposed AOMP works well for wide range of SNRs and various levels of spectrum occupancies. Numerically, AOMP offers an average NMSE improvement of 2.12%, 24.09% and 29.70% over MOMP, MUSIC and GPABP, respectively. In the next chapter, cumulant based automatic modulation classifier is designed to detect the modulation scheme of received signal from its non-uniformly sampled version.

Chapter 4

Automatic Modulation Classifier for Non-Uniformly Sampled Wideband Signal

In dynamic spectrum environment, radio terminal adapts its transmission parameters like frequency band, modulation scheme, sampling rate etc. according to the channel quality. Hence, multi-standard wireless communication receivers (MWCRs) capable of digitizing wideband signal and employing complete digital signal approach to identify the transmission parameters of received signal are desired. As MWCR uses non-uniform sampling (NUS) for the digitization of wideband signal, therefore, NUS based automatic modulation classifier (AMC) is required for the detection of modulation scheme. In this chapter, cumulant based AMC is designed to identify the modulation scheme such as BPSK, QPSK, 16-QAM and 64-QAM of non-uniformly sampled and subsequently reconstructed signal.

4.1 Automatic Modulation Classifier

The block diagram of AMC is shown in Fig. 4.1 and consists of four operations which are:

1. Digitization of received modulated signal via NUS technique.
2. Reconstruction of signal from non-uniform samples.
3. Features extraction from the reconstructed signal.
4. Detection of modulation scheme with the help of machine learning classification algorithm.

Next, system model of received wideband signal followed by description of each classification step is discussed.

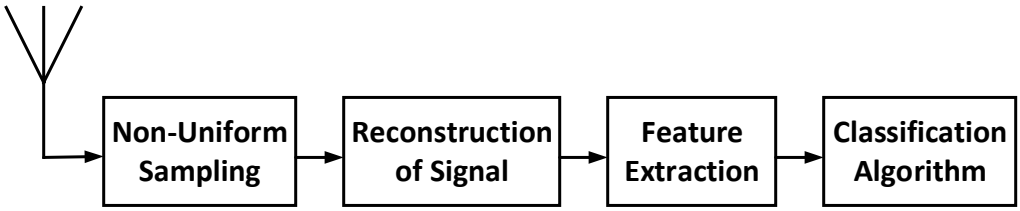

Figure 4.1: Block diagram of NUS based AMC

4.1.1 System Model

We assume that the received wideband signal at MWCR takes the following form

$$x(t) = \sum_{n=-\infty}^{\infty} Ag(t - nT + t_0)s(t)e^{(j2\pi f_c t + \theta_0)} + n(t) \tag{4.1}$$

where A is the amplitude of the received signal, $g(t) = sinc(t/T)\frac{cos(\pi\beta t/T)}{1-4\beta^2 t^2/T^2}$ is the impulse response of root raised cosine pulse shaping filter with β roll off factor, T is the symbol period, t_0 is time offset, f_c is carrier frequency, θ_0 is phase offset, $n(t)$ is additive white Gaussian noise and $s(t)$ is the modulated symbol which is

$$s(t) = \begin{cases} e^{j2\pi(m-1)/M} & \text{for M-PSK,} \\ a_m + jb_m & \text{for M-QAM} \end{cases} \tag{4.2}$$

where M is the order of the modulation scheme and $m \in \{1, 2, ..., M\}$ is the m^{th} symbol. Here, t_0 and θ_0 are assumed to be zero.

For NUS based classification, the received signal, $x(t)$ is first digitized by NUS techniques discussed in Chapter 2. Thereafter, the signal is reconstructed back from non-uniform samples with the help of support generated from reconstruction techniques (discussed in Chapter 2 and Chapter 3). Next, modulation classification is applied on the reconstructed signal which consists of two steps: 1) Extraction of features from the signal, and 2) Application of machine learning classification algorithms.

4.1.2 Modulation Classifier

For feature extraction, we used fourth and sixth order cumulants of reconstructed signal, $y(t)$. Cumulants are made up of moment of $y(t)$. For complex valued signal, fourth and sixth order cumulants are given as,

1. $C_{40} = M_{40} - 3M_{20}^2$
2. $C_{41} = M_{40} - 3M_{20}M_{21}$
3. $C_{42} = M_{42} - |M_{20}|^2 - M_{21}^2$

4. $C_{60} = M_{60} - 15M_{20}M_{40} + 20M_{20}^3$

5. $C_{61} = M_{61} - 5M_{21}M40 - 10M_{20}M_{41} + 30M_{20}^2M_{21}$

6. $C_{62} = M_{62} - 6M_{20}M_{42} - 8M_{21}M_{41} - M_{22}M_{40} + \quad 6M_{20}^2M_{22} + 24M_{21}^2M_{20}$

7. $C_{63} = M_{63} - 9M_{21}M_{42} + 12M_{21}^3 - 3M_{20}M_{43} - 3M_{22}M_{41} + 18M_{20}M_{21}M_{22}$

where $M_{pq} = E[y(t)^{p-q}(y^*(t))^q]$ is the moment of the signal $y(t)$.

After the generation of features, machine learning classification algorithm is used for classifying modulation schemes. Classification algorithm works in two phases: 1) Training Phase, and 2) Testing Phase. Training phase generates the trained model of classifier with the help of extracted features. Then, from the trained model and features of currently received signal, testing phase finds the modulation scheme of the received signal.

4.2 Simulation Results

In this section, simulation results for analyzing the performance of AMC for wide range of SNRs and spectrum occupancies are presented.

To begin with, average classification accuracy of AMC designed using two different machine learning classifiers is shown in Fig. 4.2. These classifiers are: 1) K-nearest neighbor (KNN), and 2) Support vector machine (SVM) with radial basis function (RBF) kernel. Here, we have considered proposed AOMP approach for reconstruction. Wideband signal used in the observation has 19.74% spectrum occupancy. SVM classifier is implemented by libsvm [25] tool. Please refer to [25] for detailed description of parameters used for implementing SVM classifier. For the implementation of KNN, the parameter K is taken as 23.

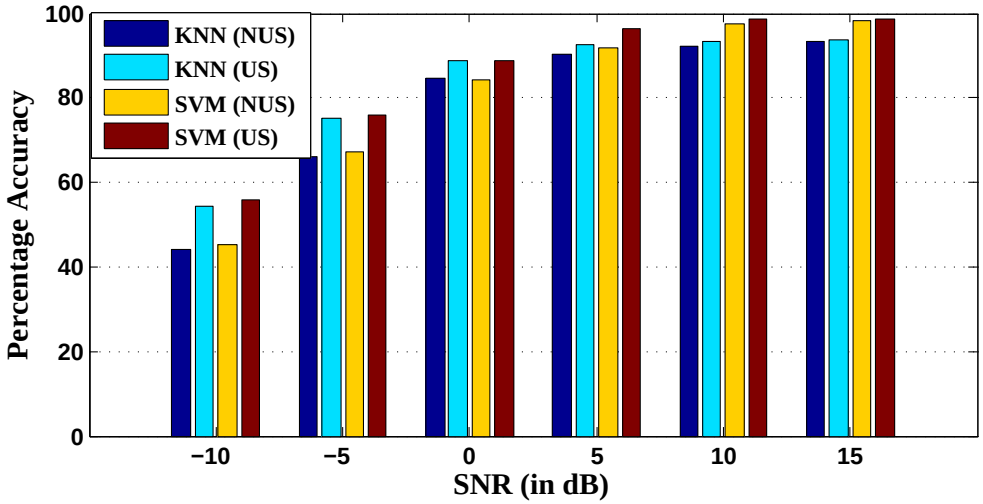

Figure 4.2: Average classification accuracy by SVM and KNN classifiers

From Fig. 4.2, it can be observed that the classification accuracy for NUS approaches to that of uniform sampling (US) at high SNR. Furthermore, SVM classifier performs better than KNN classifier for both US and NUS. Hence, the discussion in this section is limited to SVM classifier.

Next, the performance comparison of different reconstruction approaches for AMC application is done. Let us consider wideband signal with spectrum occupancy of 11.28%. For wide range of SNRs, modulation classification accuracy of different reconstruction approaches is given in Table 4.1. It can be observed that the proposed blind AOMP reconstruction approach performs slightly better than MOMP, MUSIC and EOMP reconstruction approaches. Henceforth, AOMP reconstruction approach is considered for NUS based classification.

Table 4.1: Average classification accuracy for different reconstruction approaches

SNR (in dB)	**NUS**				**Uniform Sampling**
	MOMP, [14]	**MUSIC, [13]**	**EOMP, [17]**	**AOMP**	
-10	49.92	48.69	48.45	49.92	63.92
-5	72.96	70.14	70.16	72.96	84.48
0	87.33	85.86	85.66	87.33	94.06
5	94.15	93.42	93.66	94.96	97.52
10	97.78	97.39	97.62	97.83	98.61
15	98.35	98.55	98.61	98.82	98.85
25	98.81	98.74	98.64	98.85	99.02

Average classification accuracy for different modulation schemes over a wide range of SNRs is shown in Fig. 4.3. A wideband signal consisting of only one active frequency band is used here. It can be observed that for NUS, classification accuracy of BPSK and QPSK modulation schemes is almost 100% and equal to that for US at a SNR of 0dB and 5dB respectively. Similarly, for 16-QAM and 64-QAM modulation schemes, classification accuracy for NUS is almost 99% and equal to that for US at a SNR of 15dB.

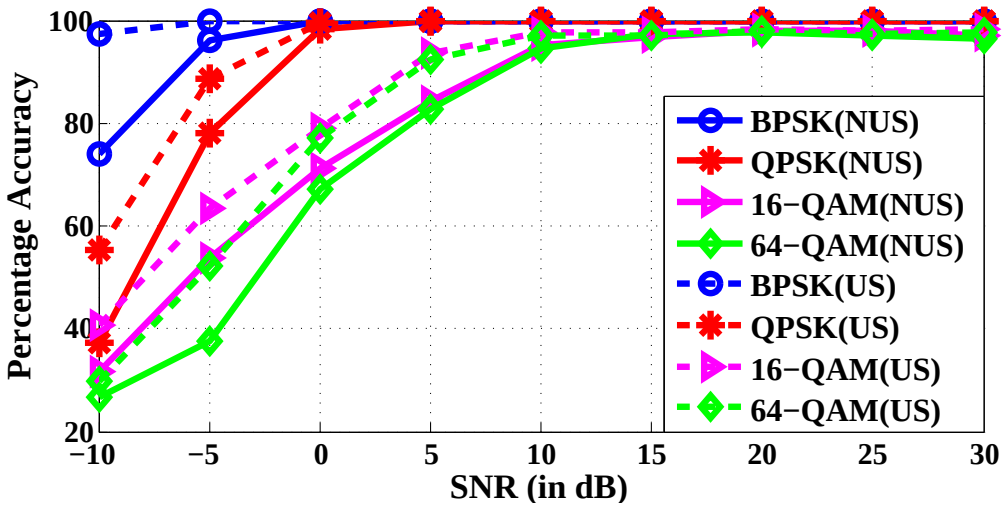

Figure 4.3: Average classification accuracy for different modulation schemes

Average classification accuracy for various levels of sparsity over a wide range of SNRs is shown in Fig. 4.4. It can be observed that a multiband signal of 2.8% sparsity can achieve the classification accuracy of around 99% at SNR of 0dB whereas the same accuracy can be achieved by 11.28% and 19.74% sparse signal at SNR of 15dB.

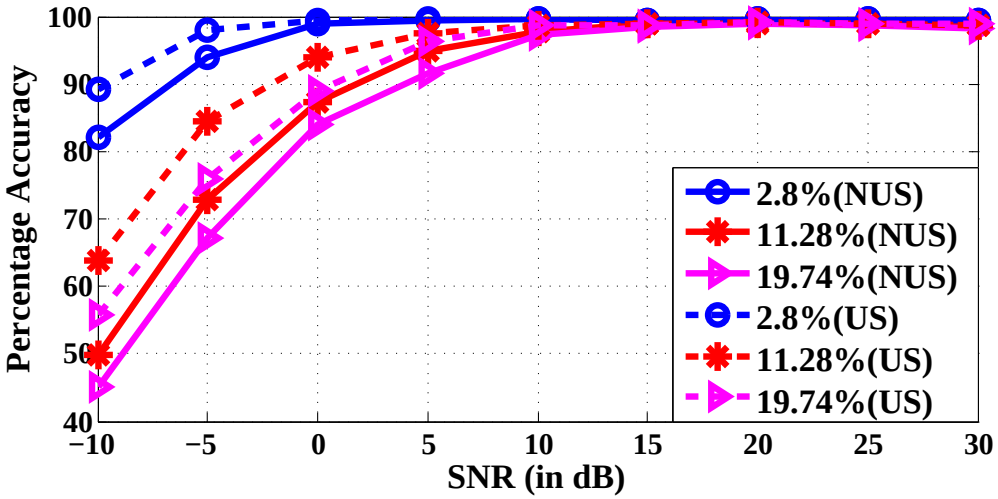

Figure 4.4: Average classification accuracy for various levels of sparsity

4.3 Summary

In this chapter, cumulant and machine learning algorithm based automatic modulation classifier (AMC) is designed to classify BPSK, QPSK, 16-QAM and 64-QAM modulation schemes. Classification is performed for either uniformly sampled signal or non-uniformly sampled and subsequently reconstructed signal. Average classification accuracy for different reconstruction techniques, classification algorithms and various levels of sparsity is calculated for wide range of SNRs. It is observed that support vector machine (SVM) classifier of radial basis function kernel performs better than K-nearest neighbor classifier. Furthermore, NUS based AMC, achieves maximum average classification accuracy of around 99% for SVM classifier. In the next chapter, an USRP testbed is developed to classify modulation schemes using real radio signal.

Chapter 5

Testbed and Experimental Analysis of Automatic Modulation Classifier for Non-Uniformly Sampled Signal

In this chapter, Universal Software Radio Peripheral (USRP) testbed has been developed to analyze the performance of cumulant based automatic modulation classifier (AMC) in real radio environment. In the proposed testbed, classification of modulation schemes is performed on both uniformly sampled signal and signal reconstructed from non-uniform samples. Later, performance analysis of AMC is presented for various machine learning classifiers, antenna gains and various distances between transmitter and receiver.

5.1 Proposed USRP Testbed for AMC

In this section, the proposed USRP testbed for AMC is presented. As shown in Fig. 5.1, the proposed testbed consists of two USRPs (specifically NI USRP-2921 with VERT2450 antenna) for the realization of wireless link and two laptops for baseband signal processing. The important parameters chosen for the experimental results are given in Table 5.1. Next, the transmitter and receiver are explained in detail.

Table 5.1: Parameters of transmitter and receiver USRP

Parameters	**Transmitter**	**Receiver**
Carrier Frequency	2.5GHz	2.5GHz
IQ Sampling Rate	500ksps	500ksps
Antenna Gain	6dB	0/6/12dB
Symbol Rate	125ksps	125ksps
Acquisition Duration	NA	1s

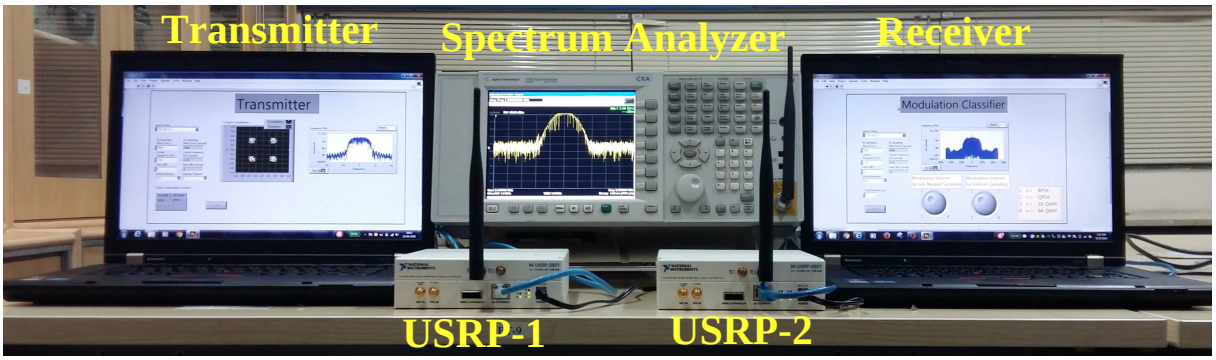

Figure 5.1: Proposed USRP testbed realizing cumulants and machine learning based AMC.

5.1.1 Transmitter

The task of the transmitter is to appropriately modulate the desired data, pulse shape the modulated symbols and perform necessary sample rate conversions followed by transmission over the desired center frequency. The chosen design environment for the transmitter is LABVIEW from National Instruments. As shown in Fig. 5.2, transmitter consists of three sub-blocks: 1) First block configures the parameters such as carrier frequency, IQ sampling rate, antenna gain and transmission port, 2) Second block modulates the data, performs pulse shape filtering on the modulated symbols and adds pilot symbols to the frame based on the parameters given by user, 3) Third block continuously transmits the modulated and filtered signal over the desired carrier frequency via USRP.

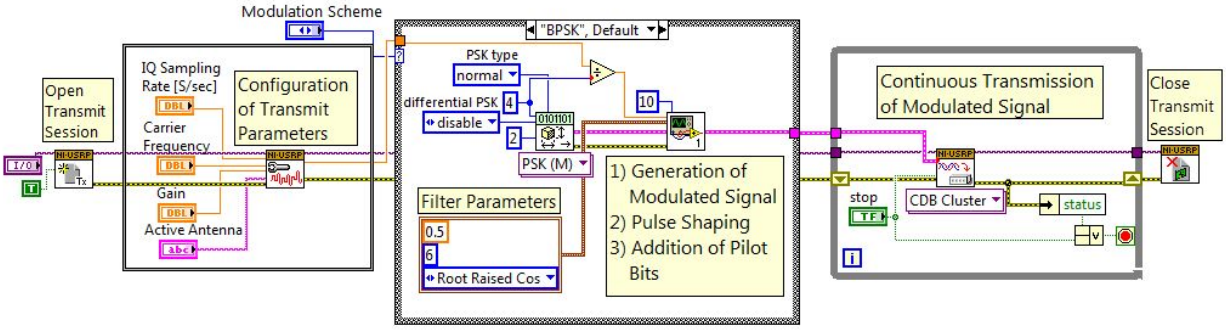

Figure 5.2: Block diagram of the transmitter

Synchronization between the transmitter and receiver is critical and one of the challenging task of the proposed testbed. As shown in Fig. 5.3, synchronization is achieved by adding the pilot symbols in each frame.

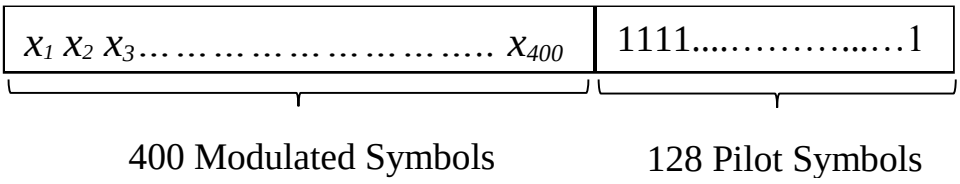

Figure 5.3: Transmission frame structure with pilot symbols for synchronization between transmitter and receiver

5.1.2 Receiver

The task of the receiver, shown in Fig. 5.4, includes transmitted signal reception using synchronization symbols, appropriate sampling and reconstruction followed by AMC. The chosen design environment for receiver is LABVIEW with MATLAB script. Similar to the transmitter, receiver parameters, given in Table 5.1, are configured in the beginning. Then, the analog signal received by an antenna is digitized using ADC at sampling rate of 100Msps followed by digital down conversion. In this way, USRP continuously produces uniformly sampled signal at Nyquist rate.

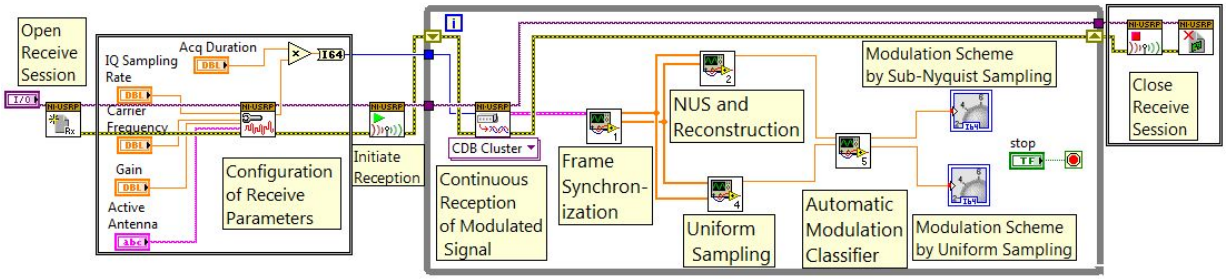

Figure 5.4: Block diagram of the receiver

Next step is the frame synchronization followed by the generation of uniform and non-uniform modulated samples. Frame synchronization is performed during the continuous reception of uniform samples to detect the beginning of frame. When pilot symbols of the received uniform samples coincide with pilot symbols then correlation will be maximum indicating the beginning of the modulated symbols. In the case of uniform Nyquist rate sampling, the detected modulated symbols are directly passed to AMC. Otherwise, symbols are passed to MCS and reconstruction blocks.

MCS is defined by two parameters, L and p where p is the number of ADCs with sampling rate L times lower than the Nyquist rate. For $c_i(t) \in \{1, 2, 3, ..., L\}$, i^{th} active coset, $x_i(n)$, containing $W = \frac{N}{L}$ samples, can be obtained from uniformly sampled signal of length N as

$$x_i(n) = x(nT) \sum_{m \in Z} \delta(n - (mL + c_i)) \qquad 0 \leq i < p \tag{5.1}$$

In order to emulate MCS using USRP, samples are appropriately chosen from Nyquist rate samples using Eq. 5.1. These active cosets are then passed to the reconstruction block.

Discrete time Fourier transform of multi-cosets is used to reconstruct the signal. This reconstruction problem is infinite dimensional problem and can be converted into finite dimensional problem by discrete multi-cosets [6]. It can be represented as

$$\mathbf{Y} = \mathbf{A}\mathbf{X} \tag{5.2}$$

where $\mathbf{Y} \in \mathbb{C}^{p \times W}$ is a product of DFT of non-uniform samples and corresponding delay, $\exp\left[-\frac{2\pi j.c_i.(w-1)}{LW}\right]$, $\mathbf{A}$ is $p \times L$ measurement matrix with element given by,

$$\mathbf{A}_{i,l} = \frac{1}{L.T} \exp\left[j\frac{2\pi}{L}.c_i.(l-1)\right] \tag{5.3}$$

and $\mathbf{X}$ is $L \times W$ matrix of DFT of uniform samples.

There are many compressive sensing algorithms which can reconstruct $\mathbf{X}$ of Eq. 5.2. In this demonstration, we used MOMP algorithm [14] which is one of the most popular algorithm.

Next step is to determine the modulation scheme of the received signal using AMC. An input to the AMC is either uniformly sampled or non-uniformly sampled and subsequently reconstructed signal. It consists of two steps: 1) Extraction of features from samples, and 2) Identification of modulation scheme with the help of classification algorithm. Here, 4^{th} and 6^{th} order cumulants based features are extracted from the samples. Please refer to [24] for more details. These features are given to machine learning classifier which then identifies the modulation type of the received signal. We have implemented two classifiers: 1) Support vector machine (SVM) with radial basis function (RBF) kernel, and 2) K-nearest neighbors (KNN). Both classifiers work in two phases: 1) Training phase, and 2) Testing phase. In the training phase, extracted features are used to generate trained model of the classifier. Then, the trained model and features of currently received signal are used in testing phase to detect the modulation scheme of the received signal.

5.2 Experimental Results

In this section, experimental results of AMC for uniformly and non-uniformly sampled signal using the proposed testbed are presented. The received signal is assumed to have around 40% sparsity. Four different modulation schemes, BPSK, QPSK, 16-QAM and 64-QAM, are considered. The parameters, L and p, of MCS are 19 and 6, respectively. Libsvm based SVM classifier and KNN classifier with 23 nearest neighbor are used for AMC. Please refer [25] for detailed description of method and parameters used for implementing SVM classifier. The training phase generates the trained model of classifier using 400 samples of each modulation scheme.

In Table 5.2, average accuracy of AMC is shown for different receiver gain, classifiers and various distances between transmitter and receiver. The performance of SVM is slightly better than KNN and average accuracy improves with the increase in receiver gain. Furthermore, performance of AMC does not degrade significantly with NUS. In Fig. 5.5, distribution of features for

QPSK and 64-QAM is shown. It can be observed that features are more spread in case of NUS compared to uniform sampling which leads to lower accuracy in the former compared to latter.

Table 5.2: Average percentage accuracy of AMC by NUS and US

Modulation Classifier	Receiver Gain	Average Percentage Accuracy							
		Distance = 1.2m		Distance = 4.2m		Distance = 8.7m		Distance = 10.2m	
		NUS	Uniform	NUS	Uniform	NUS	Uniform	NUS	Uniform
SVM	0dB	74	81.25	61	71.87	58.5	63.75	42.5	53
	6dB	75	82	61.5	73	61	67	52.62	59.5
	12dB	79.62	85.75	65.63	73.37	64.5	68.5	56.75	66
KNN	0dB	67.87	71.62	58.75	67	52.5	59.5	39	49.38
	6dB	69.5	74.5	59	67	54.5	62.75	46.38	55.5
	12dB	73.87	82.25	61.25	67.25	58	66.5	50.38	60.12

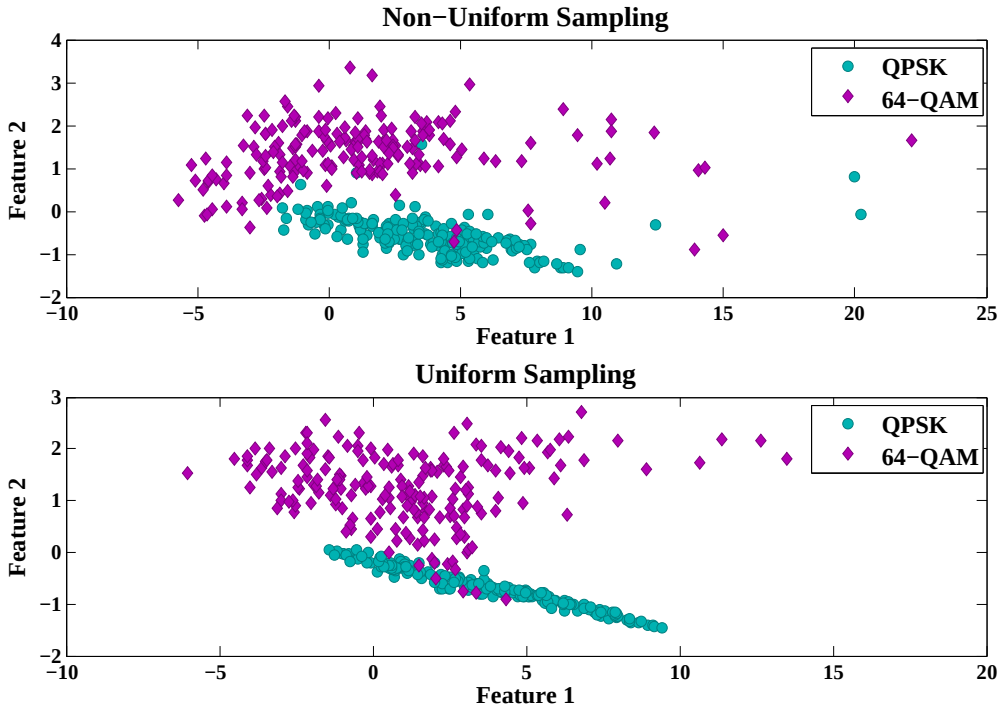

Figure 5.5: AMC using cumulant based features for uniformly and non-uniformly sampled signal

5.3 Summary

In this chapter, an USRP testbed to validate the performance of non-uniform sampling (NUS) based automatic modulation classifier (AMC) using real radio signals is developed. Performance analysis of average percentage accuracy for various modulation schemes, antenna gain and various distance between transmitter and receiver is also done. The experimental results showed that the performance of AMC does not degrade significantly with NUS given that received signal is sparse in frequency.

Chapter 6

Conclusion and Future Works

This chapter presents a brief summary of work done in this thesis. Some future works linked to the same field of research are also identified.

6.1 Conclusion

In this thesis, a low complexity adaptive orthogonal matching pursuit (AOMP) reconstruction approach has been proposed to blindly reconstruct the wideband sparse signal from non-uniformly sampled signal. Use of upper confidence bound (UCB) algorithm and normalized SNR make AOMP reconstruction approach blind and adaptive to dynamic spectrum. Simulation results show that the proposed AOMP works well for wide range of SNRs and spectrum occupancies. Numerically, AOMP offers an average improvement of 2.12%, 24.09% and 29.70% in NMSE over multi-variate OMP (MOMP), multiple signal classification (MUSIC) and greedy pursuits assisted basis pursuits (GPABP), respectively.

Furthermore, cumulant and machine learning algorithm based automatic modulation classifier (AMC) is designed to identify modulation scheme of the received signal from its non-uniformly sampled version. Simulation results show that the classification accuracy of blind AOMP reconstruction approach is better than that of other reconstruction approaches. Performance comparison is also made for uniformly sampled and non-uniformly sampled signal. It is observed that classification accuracy achieved by non-uniform sampling (NUS), approaches to that of uniform sampling with increase in SNR. To evaluate the performance of AMC in real radio environment, an universal software radio peripheral (USRP) testbed has been developed. The experimental results show that the performance of AMC does not degrade significantly with NUS given that signal is sparse in frequency.

6.2 Future works

Some future works to purse research in this area are identified as :

- **Blind Reconstruction of Individual Band of Multiband Signal**
  Proposed reconstruction technique, reconstructs all frequency bands of wideband signal. But MWCR based radio terminal generally processes information received over single frequency band. An extension of proposed blind reconstruction approach for single frequency band reconstruction can significantly reduces the computational complexity of baseband signal processing algorithms.

- **USRP Testbed for Adaptive AMC**
  Developed USRP testbed for AMC employs MOMP reconstruction approach. MOMP approach uses spectrum information for the reconstruction and hence, can not be used under dynamic spectrum environment. For making the testbed adaptive to dynamic spectrum, an online learning algorithm can be integrated in the proposed USRP testbed.

- **USRP Testbed for MIMO Systems**
  Proposed AMC testbed works on a conventional single carrier modulated signal. However, multi-carrier waveforms such as OFDM, filtered OFDM, GFDM, FBMC are being considered for 5G. Further extension of the proposed testbed includes performance analysis with these waveforms along with MIMO systems.

Bibliography

[1] J. Wang, M. Ghosh and K. Challapali, "Emerging Cognitive Radio Applications: A Survey," *IEEE Communications Magazine*, vol. 49, no. 3, pp. 74-81, March 2011.

[2] J. Palicot, H. Zhang and C. Moy, "On The Road towards Green Radio," *URSI Radio Science Bulletin*, no. 347, pp. 4056, Dec. 2013.

[3] S. J. Darak and A. P. Vinod, "Design of Low Complexity Variable Digital Filters and Recongurable Filter Banks for Multi-Standard Wireless Communication Receivers," PhD Thesis, NTU Singapore, 2013

[4] R. Venkataramani and Y. Bresler, "Sub-Nyquist sampling of multiband signals: perfect reconstruction and bounds on aliasing error," *IEEE International Conference on Acoustics, Speech and Signal Processing*, pp. 1633 - 1636, Seattle, Washington, May 1998.

[5] R. Venkataramani and Y. Bresler, "Optimal non-uniform non-uniform sampling and reconstruction for multiband signals," *IEEE Transactions on Signal Processing*, vol. 49, no. 10, pp. 2301-2313, Oct. 2001

[6] R. Grigoryan, T. L. Jensen, T. Arildsen and T. Larsen, "Reducing the Computational Complexity of Reconstruction in Compressed Sensing Nonuniform Sampling," in *Proceedings of the 21st European Signal Processing Conference (EUSIPCO)*, pp. 1-5, Marrakech, Morocco, Sept. 2013.

[7] M. Mishali and Y. C. Eldar, "From theory to practice: Sub-Nyquist sampling of sparse wideband analog signals," *IEEE Journal of Selected Topics in Signal Processing*, vol. 4, no. 2, pp. 375-391, April 2010.

[8] P. Feng and Y. Bresler, "Spectrum-blind minimum-rate sampling and reconstruction of multiband signals," *IEEE International Conference on Acoustics, Speech and Signal Processing*, pp. 1688-1691, Atlanta, GA, May 1996

[9] R. Venkataramani and Y. Bresler, "Perfect reconstruction formulae and bounds on aliasing error in nonuniform nonuniform sampling of multiband signals," *IEEE Transactions on Information Theory*, vol. 46, no. 6, pp. 2173-2183, Sep. 2000.

[10] M. Mishali and Y. C. Eldar, "Blind Multiband Signal Reconstruction: Compressed Sensing for Analog Signals,"in *IEEE Transactions on Signal Processing*, vol. 57, no. 3, pp. 993-1009, March 2009.

[11] M. Rashidi, K. Haghighi, A. Owrang and M. Viberg, "A wideband spectrum sensing method for cognitive radio using sub-nyquist sampling," *IEEE International Digital Signal Processing and Signal Processing Education Workshop*, pp. 30-35, Sedona, AZ, Jan. 2011.

[12] M. Rashidi, K. Haghighi, A. Panahi and M. Viberg, "A NLLS based sub-nyquist rate spectrum sensing for wideband cognitive radio," *IEEE Symposium on New Frontiers in Dynamic Spectrum Access Networks (DySPAN)*, pp. 545 - 551, Aachen, Germany, May 2011.

[13] Y. Bresler, "Spectrum-blind Sampling and Compressive Sensing for Continuous-index Signals," *Information Theory and Applications Workshop*, pp. 547554, San Diego, California, Jan. 2008.

[14] Joel A. Tropp and A. C. Gilbert, "Signal Recovery From Random Measurements Via Orthogonal Matching Pursuit," *IEEE Transactions on Signal Processing*, vol. 53, no. 12, Dec. 2007

[15] T. Zhang, "Sparse Recovery With Orthogonal Matching Pursuit Under RIP," *IEEE Transactions on Information Theory*, vol. 57, no. 9, pp. 6215-6221, Sept. 2011.

[16] S. Narayanan, S. K. Sahoo and A. Makur, "Greedy Pursuits Assisted Basis Pursuit for Compressive Sensing," *European Signal Processing Conference*, pp. 694-698, Nice, France, Aug. 2015.

[17] S. K. Sahoo and A. Makur, "Signal recovery from random measurements via extended orthogonal matching pursuit," *IEEE Transactions on Signal Processing*, vol. 63, no. 10, pp. 2572-2581, May 2015.

[18] N. Vaswani and W. Lu, "Modified-CS: Modifying compressive sensing for problems with partially known support," *IEEE Transactions on Signal Processing*, vol. 58, no. 9, pp. 4595-4607, Sept. 2010.

[19] E. Candes and T. Tao, "Decoding by linear programming ," *IEEE Transactions on information Theory*, vol. 51, no. 12, pp. 4203-4215, Dec. 2005

[20] M. Rudelson and R. Vershynin, "Sparse reconstruction by convex relaxation: Fourier and Gaussian measurements," *IEEE Conference on Information Sciences and Systems*, pp. 207-212, Princeton, New Jersey, March 2006.

[21] P. Auer, N. Cesa-Bianchi, and P. Fischer, "Finite-time Analysis of the Multiarmed Bandit Problem," *Machine Learning*, vol. 47, no. 2, pp. 235-256, May 2002.

[22] S. J. Darak, C. Moy, H. Zhang and J. Palicot, "Dynamic Spectrum Access with Tunable Bandwidth for Multi-standard Cognitive Radio Receivers," in *Proc.* 37^{th} *International Conference in Telecommunications and Signal Processing*, pp. 1-5, Berlin, Germany, July 2014.

[23] Zhechen Zhu and Asoke K. Nandi ,"Automatic Classification of Digital Communication Signa Modulations," PhD Thesis, Brunel University London, 2014.

[24] M. W. Aslam, Z. Zhu and A. K. Nandi, "Automatic Modulation Classification Using Combination of Genetic Programming and KNN," *IEEE Transactions on Wireless Communications*, vol. 11, no. 8, pp. 2742-2750, Aug. 2012.

[25] C. C. Chang and C. J. Lin, "LIBSVM: A Library for Support Vector Machines," *ACM Transactions on Intelligent Systems and Technology*, vol. 2, no. 3, pp. 27, April 2011. Software available at http://www.csie.ntu.edu.tw/ cjlin/libsvm.